MESON CLOUD IN THE NUCLEON
AND SEARCH FOR $\bar{u}$-$\bar{d}$ ASYMMETRY*†

A. SZCZUREK[a,b] AND H. HOLTMANN[a]

[a] Institut für Kernphysik, Forschungszentrum Jülich
W-5170 Jülich, Federal Republic of Germany
[b] Institute of Nuclear Physics
PL-31-342 Krakow, Poland

Mesonic models predict violation of SU(2) symmetry in the nucleon sea which seems to be necessary to explain the violation of the Gottfried Sum Rule. Careful analysis of the Drell–Yan processes in p-p and p-n collisions should provide complementary data to the Gottfried Sum Rule on the $\bar{d}/\bar{u}$ asymmetry. Large one-loop corrections in semileptonic hyperon decays can be compensated by a tiny shift in the values of D and F. The meson cloud is an important ingredient in understanding the spin structure of the nucleon.

PACS numbers: 14.20. Dh, 13.60. Hb, 11.50. Li, 13.30. Ce

1. Introduction

It has been customarily assumed that the nucleon sea is flavor symmetric $(\bar{d}_p(x) = \bar{u}_p(x))$. There is no general principle that forces one to this hypothesis other than the fact that it appears as a natural consequence of a perturbative approach to the nucleon's parton distributions. There is no justification for such a restricted point of view to proton structure and there is strong indication that nonperturbative physics is crucial. Specifically, the observed violation of the Gottfried Sum Rule (GSR) [1] provides experimental evidence that the nucleon sea is not flavor symmetric. There remains no quantitatively compelling explanation for the effect.

The meson cloud model provides a natural explanation for the excess of $\bar{d}$ over $\bar{u}$ quarks already in its simplest form in which the proton contains

---

components of a bare proton and π^0 and a bare neutron and π^+. In this presentation we review a generalization of this simple idea, developed recently in Jülich. We discuss the role of the meson cloud in deep-inelastic lepton scattering, especially in connection with the GSR and present predictions for the nucleon–nucleon induced dilepton production at high energies. In addition, we discuss the one-loop meson corrections in the semileptonic hyperon decays and for the spin structure of the nucleon.

2. Gottfried sum rule

The GSR addresses the value of the integral over x of the difference of the $F_2(x)$ structure function of the proton (p) and neutron (n). It is written[1] as

$$\int_0^1 \left[F_2^p(x) - F_2^n(x) \right] \frac{dx}{x}$$

$$= \frac{1}{3} \int_0^1 \left(\left[u_p^v(x) - d_p^v(x) \right] + 2 \left[\overline{u}_p(x) - \overline{d}_p(x) \right] \right) dx , \quad (1)$$

where $u_p^v(x) \equiv u_p(x) - \overline{u}_p(x)$, etc., and charge symmetry has been assumed, i.e., $u_p(x) = d_n(x)$, etc. If one further makes the customary assumption that $\overline{u}_p(x) = \overline{d}_p(x)$, then

$$\int_0^1 \left[F_2^p(x) - F_2^n(x) \right] \frac{dx}{x} = \frac{1}{3} . \quad (2)$$

Equation (2) is referred to as the GSR. However the most recent measurement [2] of the relevant structure functions over the interval $0.004 \le x \le 0.8$ yields, when extrapolated to $0 \le x \le 1$,

$$\int_0^1 \left[F_2^p(x) - F_2^n(x) \right] \frac{dx}{x} = 0.24 \pm 0.016 , \quad (3)$$

at $Q^2 = 5 \text{ GeV}^2$.

---

[1] The structure functions $F_2(x)$ are functions of Q^2, as are the quark distribution functions $q(x)$. The Q^2 dependence is suppressed to keep the expressions from being too cumbersome.

Taken at face value, a comparison of Eqs (1), (2), and (3) implies

$$\int\limits_0^1 \left[\, \overline{d}_p(x) - \overline{u}_p(x) \right] dx = 0.135 \pm 0.024 \,, \tag{4}$$

in marked disagreement with the customary assumption. It appears impossible [3] to generate such a large difference in the $\overline{d}$ and $\overline{u}$ distributions from perturbative processes; hence, the answer likely lies with more complicated nonperturbative physics. For example, there have been a few [4–10] attempts to calculate the difference due to virtual meson emission. In the absence of such calculations, all that can be done is to reparametrize the $\overline{u}_p(x)$ and $\overline{d}_p(x)$ distributions so that they agree with the observed violation of the GSR.

Typically one defines

$$\overline{d}_p(x) = \overline{q}(x) + \frac{\Delta(x)}{2} \tag{5}$$

and

$$\overline{u}_p(x) = \overline{q}(x) - \frac{\Delta(x)}{2} \,, \tag{6}$$

where

$$\int\limits_0^1 \Delta(x) dx = 0.135 \pm 0.024 \,. \tag{7}$$

The initial reparametrization [11] used $\Delta(x) = A(1 - x)^k$, which placed the $\overline{d}$-$\overline{u}$ difference at large x ($x > 0.05$) and led to very large values for $\overline{d}_p(x)/\overline{u}_p(x)$ for $x \geq 0.1$. These large ratios have been ruled out by a recent reanalysis of earlier Drell–Yan data. More recent [12] parametrizations have a form $\Delta(x) = B(1 - x)^\ell/x^{0.5}$, which places the bulk of the difference at smaller x.

3. Hybrid meson-baryon model of the nucleon

In this section we briefly review a recent hybrid meson-baryon model of the nucleon [10] and present its prediction for the asymmetry of the light sea antiquarks. In this model the nucleon is viewed as a quark core, termed a bare nucleon, surrounded by the mesonic cloud. The nucleon wave function can be schematically (we neglect the isospin degrees of freedom for simplicity) written as a superposition of a few principle Fock components

$$|N\rangle_{\text{dressed}} = Z^{1/2} \left[|N\rangle_{\text{bare}} + \alpha |N\pi\rangle + \beta |\Delta\pi\rangle + (\ldots) \right] . \tag{8}$$

The factor Z measures the probability that the physical nucleon contains a bare nucleon. The model of Ref. [10] includes all the mesons required in the description of the low energy nucleon–nucleon and hyperon–nucleon scattering. Furthermore it ensures charge conservation, number and momentum sum rules.

The x-dependence of the structure functions in the meson cloud model can be written as a sum of components corresponding to the expansion given by Eq. (8).

$$F_2^N(x) = Z \left[F_{2,\text{core}}^N(x) + \sum_{MB} \left(\delta^{(M)} F_2(x) + \delta^{(B)} F_2(x) \right) \right] . \qquad (9)$$

The contributions from the virtual mesons and baryons can be written as a convolution of the meson (baryon) structure functions and its longitudinal momentum distribution in the nucleon

$$\delta^{(M)} F_2(x) = \int\limits_x^1 dy f_M(y) F_2^M \left(\frac{x}{y} \right) . \qquad (10)$$

Equation (10) can be written in an equivalent form in terms of the quark distribution functions

$$x \delta^{(M)} q_f(x) = \int\limits_x^1 dy f_M(y) \left(\frac{x}{y} \right) q_f^M \left(\frac{x}{y} \right) . \qquad (11)$$

The longitudinal momentum distributions of virtual mesons (or baryons) can be calculated assuming a model of the vertex, and depends on the coupling constants and form factors. For the dominant contributions $(\pi N, \pi \Delta)$ they are given by simple formulas

$$f_{\pi(N)}(y) = \frac{3 g_{N\pi N}^2}{16\pi^2} y \int\limits_{-\infty}^{t^{\max}} dt \frac{[G(t)]^2}{(t - m_\pi^2)^2} (-t) , \qquad (12)$$

$$f_{\pi(\Delta)}(y) =$$
$$\frac{2 g_{N\pi\Delta}^2}{24\pi^2} y \int\limits_{-\infty}^{t^{\max}} dt \frac{[G(t)]^2}{(t - m_\pi^2)^2} [(m_N + m_\Delta) - t] \left[\frac{(m_N^2 - m_\Delta - t)^2}{4 m_\Delta^2} - t \right] . \qquad (13)$$

The main ingredients of the model are the vertex coupling constants, the parton distribution functions for the virtual mesons and baryons, and the vertex form factors which account for the extended nature of the hadrons. The coupling constants are assumed to be related via SU(3) symmetry. The measured free-hadron parton distributions are used. In Ref. [10] an overall cut-off parameter has been used for simplicity. This led to the value of 0.28 for the GSR, about $^5/_9$ of the original NMC effect. In principle the cut-off parameter can be slightly different for different components. In our model the GSR is a delicate interplay between πN and $\pi\Delta$ components and depends on their probabilities in the nucleon wave function. By lowering the probability of the $\pi\Delta$ component one could achieve a better agreement with the NMC result [2]. This is a crucial point in order to understand the NMC result and requires a more detailed analysis. Phenomenologically the $N\pi\Delta$ vertex can be determined [13] by comparison of the one pion exchange model (OPEM) with high energy data

$$(a) \qquad p(p, \Delta^{++})X\,,$$
$$(b) \qquad p(\bar{p}, \Delta^{++})X\,. \qquad (14)$$

The cross section for the p(h,B)X reaction in the OPEM can be expressed as

$$\frac{d\sigma}{dx_B dp_\perp} = \tilde{f}(x_B, p_\perp)\sigma_{h\pi}^{tot}\,, \qquad (15)$$

where $\tilde{f}(x_B, p_\perp)$ is a function which involves the $N\pi B$ form factor and $\sigma_{h\pi}^{tot}$ is the total cross section for $h\pi$ collision. While reaction (14a) involves $\sigma_{\pi^- p}^{tot}$ which is well known experimentally, reaction (14b) involves $\sigma_{\pi^-\bar{p}}^{tot}$, which can be easily related to $\sigma_{\pi^+ p}^{tot}$ — also well known. Experimentally these cross sections approximately scale in a broad range of energies, making application of OPEM very simple.

In Fig. 1 we show prediction of the OPEM with the experimental data for $p(p, \Delta^{++})X$ [14] and $p(\bar{p}, \Delta^{++})X$ [15] reactions for different values of the cut-off parameter. The data for both reactions prefer a cut-off of about 1.0 GeV in a dipole parametrization. We note that the slight energy dependence of cross sections has been disregarded here and we have taken 24 mb for the $\sigma_{\pi p}^{tot}$ cross section.

In the following we will use cut-off parameter of 1.2 GeV for the components with octet baryons and of 1.0 GeV for the components with decuplet baryons. The softer form factor for the $N\pi\Delta$ vertex than for $N\pi N$ or $NK\Lambda$ vertices seems be a universal feature of high energy scattering [16, 17].

In Fig. 2 we present the difference $x(\bar{d} - \bar{u})$ obtained in the framework of the meson cloud model and for various parametrizations with asymmetric sea-quark distributions. It is interesting to notice that the mesonic model
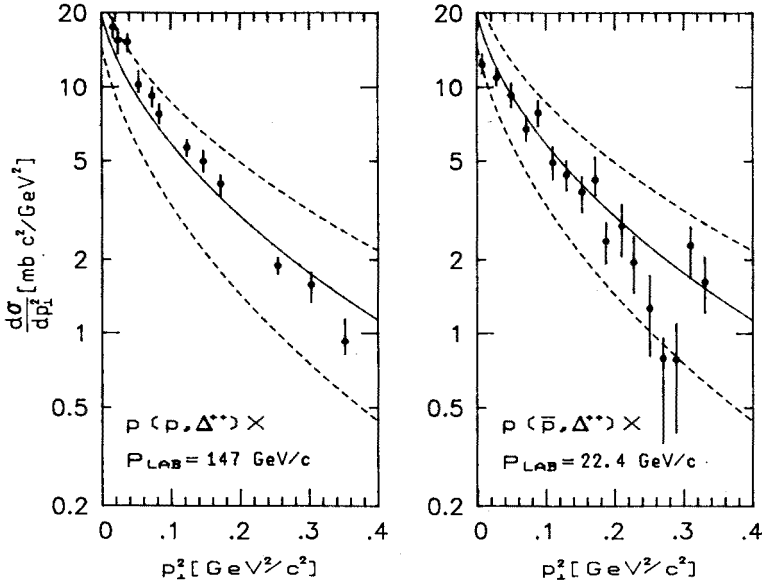
Fig. 1. Differential cross section $d\sigma/dp_T^2$ as a function of p_T^2 for Δ^{++} production in (a) pp collision [14] measured at Fermilab and (b) $\bar{p}p$ collision [15] measured at Serpukhov. The solid line is for cut-off of 1.0 GeV, whereas the dotted lines are for 0.8 GeV and 1.2 GeV.
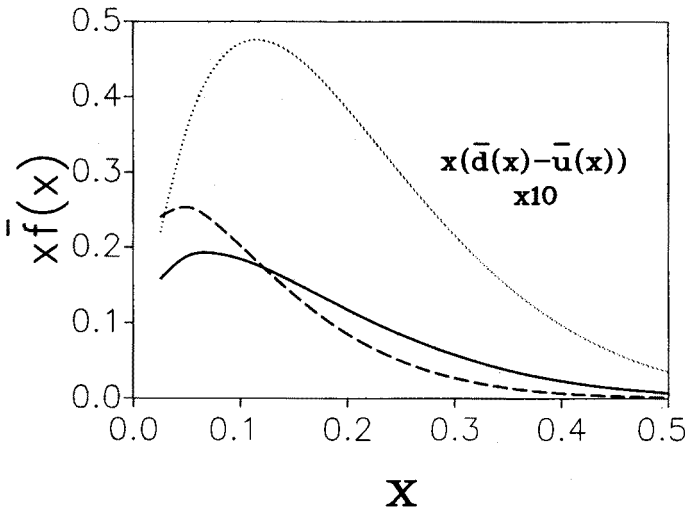

Fig. 2. The difference $x\bar{d}(x) - x\bar{u}(x)$ magnified by the factor 10. Result of the meson cloud model is shown by the solid line. We present also the difference for asymmetric phenomenological parametrizations: Eichten–Hinchliffe–Quigg [8] (dashed curve) and Martin–Stirling–Roberts [12] (dotted curve).

is qualitatively similar both in shape and magnitude to the result of a very recent global fit of Martin, Stirling and Roberts (MSR) to the world deepinelastic and Drell–Yan data [12]. For instance, the GSR obtained from our model is 0.255, with 0.235 in the experimentally measured region. This can be compared with the value of 0.26 obtained from the recent MSR fit. The Eichten–Hinchliffe–Quigg [8] and Ellis–Stirling [11] parametrizations give larger differences; however, they have been adjusted to reproduce the NMC value [2] of the GSR.

In Table I we present the contributions of each of the components in Eq. (8). One notes that only the processes involving virtual π and ρ mesons contribute to the asymmetry. The ratio $(\overline{d}(x) - \overline{u}(x))/(\overline{d}(x) + \overline{u}(x))$ turns out to be rather insensitive to the choice of parton distributions in mesons and in the bare baryons.

TABLE I

A list of the processes contributing to the violation of the $\overline{u}$-$\overline{d}$ symmetry in the nucleon sea. In addition we show also probabilities (in %) of the individual Fock components in the expansion of the nucleon wave function given by Eq. (8) and numbers of antiquarks contained in the proton wave function.

component	probability	$\overline{u}$	$\overline{d}$	$\overline{d} - \overline{u}$
bare N	59.38	—	—	—
$\pi + N$	21.15	0.0353	0.1763	0.1410
$\rho + N$	1.73	0.0029	0.0144	0.0115
$\pi + \Delta$	10.69	0.0712	0.0356	−0.0356
$\rho + \Delta$	0.30	0.0020	0.0010	−0.0010
symm. cont.	6.75	0.0256	0.0256	—
sum	100.00	0.1370	0.2529	0.1159

4. Drell–Yan processes

The Drell–Yan (DY) process with incident nucleons can be made extremely sensitive to the $\overline{d}_p(x)/\overline{u}_p(x)$ distribution in the target [11].

The Drell–Yan process [18] involves the electromagnetic annihilation of a quark (antiquark) from the incident hadron A with an antiquark (quark) in the target hadron B. The resultant virtual photon materializes as a dilepton pair $(\ell^+\ell^-)$. The cross section for the DY process can be written as

$$\frac{d\sigma^{AB}}{dx_1 dx_2} = \frac{4\pi\alpha^2}{9sx_1x_2} K(x_1, x_2) \sum_f e_f^2 \left[q_A^f(x_1)\overline{q}_B^f(x_2) + \overline{q}_A^f(x_1)q_B^f(x_2) \right] ,$$

$$(16)$$

where s is the square of the center-of-mass energy and x_1 and x_2 are the longitudinal momentum fractions carried by the quarks of flavor f. The $q_A^f(x_1)$ and $q_B^f(x_2)$ are the quark distribution functions of the beam and target, respectively. The factor $K(x_1, x_2)$ accounts for the higher-order QCD corrections that enter the process.

The valence quark distribution in the nucleon falls off as a much smaller power of $(1-x)$ than does its sea quark distribution, so that as $x \to 1$, there are only valence quarks and no sea quarks. Indeed, if x_1 is selected such that $x_1 = x_2 + 0.3$, the first term in Eq. (16) dominates the second term by a factor of more than 10. Thus, forming the ratio of the Drell–Yan yields for pp to pn, we have

$$\left. \frac{d\sigma_{\mathrm{DY}}^{pp}}{d\sigma_{\mathrm{DY}}^{pn}} \right|_{x_F > 0.3} \simeq \frac{4 u_p(x_1) \bar{u}_p(x_2) + d_p(x_1) \bar{d}_p(x_2)}{4 u_p(x_1) \bar{d}_p(x_2) + d_p(x_1) \bar{u}_p(x_2)}, \tag{17}$$

where it is assumed that $K_p(x_1, x_2) = K_n(x_1, x_2)$ and $u_p(x) = d_n(x)$, etc. In the limit $x_1 \to 1$, $\frac{d_p(x_1)}{u_p(x_1)} \to 0$, and in that limit one has

$$\left. \frac{d\sigma_{\mathrm{DY}}^{pp}}{d\sigma_{\mathrm{DY}}^{pn}} \right|_{\substack{x_F > 0.3 \\ x_1 \to 1}} = \frac{\bar{u}_p(x_2)}{\bar{d}_p(x_2)}. \tag{18}$$
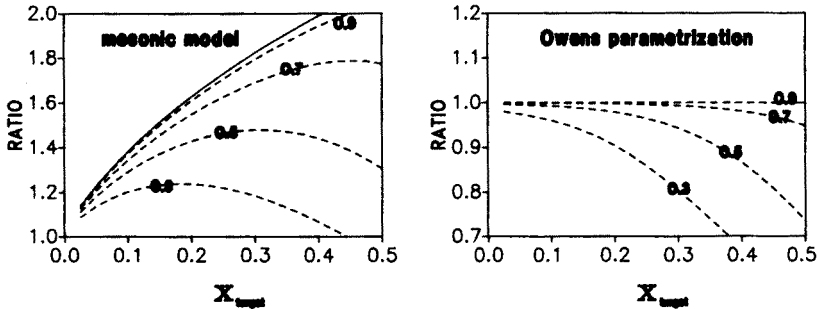

Fig. 3. (a) The ratio $\sigma_{\mathrm{DY}}^{pn}/\sigma_{\mathrm{DY}}^{pp}$ as a function of the target x_2 for selected values of the beam x_1. Predictions of the meson cloud model are shown on the left side, while the result of a phenomenological parametrization [19] with symmetric antiquark distributions is presented on the right side.

In practice this kinematical region is not accessible experimentally and a more general expression based on Eq. (16) has to be used. In Fig. 3 we present the prediction of the meson cloud model sketched in the previous section for the ratio $\sigma_{\mathrm{DY}}^{pn}(x_1, x_2)/\sigma_{\mathrm{DY}}^{pp}(x_1, x_2)$ as a function of x_2 for the expected experimental range of x_1. We also present the results obtained from

the symmetric phenomenological sea-quark distributions of Ref. [19]. As is clearly seen from the figure, the experimental ratio, larger or smaller than unity in the experimentally meaningful region $x_2 < 0.3$, should definitely discriminate between symmetric and asymmetric nucleon seas. It would also give a quantitative measure of the effect, putting further constraints on the mesonic models.
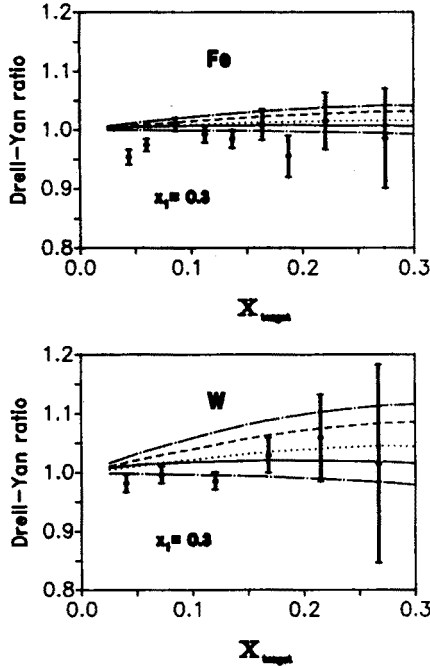

Fig. 4. The ratio $2\sigma_{DY}^{pA}/A\sigma_{DY}^{pd}$ as a function of the target x_2 for iron and natural tungsten. The experimental data are taken from Ref. [20] and Ref. [31]. Predictions of the meson-cloud model are shown by the solid line and the result with symmetric sea quark distribution by the long dashed line. Results obtained from the phenomenological parametrizations with the asymmetry built in are shown for comparison: Field–Feynman [21] (dotted curve), Eichten–Hinchliffe–Quigg [8] (dashed curve), Ellis–Stirling [11] (dash-dotted curve). Note that no nuclear effects have been included.

The ratio of the DY yield from a nucleus with $N \neq Z$ to that from an isoscalar target such as deuterium, is sensitive to the $\bar{d}_p(x) - \bar{u}_p(x)$ difference. These ratios have been measured by the E772 Collaboration at FNAL [20] for carbon, calcium, iron and tungsten targets. Elementary algebra leads to the following result:

$$\frac{2d^2\sigma_{DY}^{pA}}{Ad^2\sigma_{DY}^{pd}} = \frac{2Z}{A} + \frac{N-Z}{A}\frac{2\sigma_{DY}^{pn}(x_1,x_2)}{(\sigma_{DY}^{pp}(x_1,x_2)+\sigma_{DY}^{pn}(x_1,x_2))}, \qquad (19)$$

where Z, N, A are the number of protons, neutrons and the atomic number, respectively. In Fig. 4 we present the ratios for iron and natural tungsten targets as a function of x_2 (target) for fixed value $x_1 = 0.3$, which correspond roughly to the experimental situation. For comparison we present also the experimental data of the E772 Collaboration. In addition we show the results with the flavor symmetric sea distributions of Ref. [19]. No large difference between the result of the mesonic model and the symmetric parametrization can be seen. In our opinion the data do not select in a convincing way the symmetric vs. asymmetric distributions. We present also in Fig. 4 similar results with the flavor asymmetric sea-quark distributions of Refs [21, 11, 8]. As can be seen from the figure, the data exclude such asymmetric parametrizations.

5. Semileptonic decays of the octet baryons

The matrix elements of the current operators for the semileptonic decays of the baryons belonging to the octet can be parametrized in terms of the q^2-dependent form factors,

$$
\langle B_f | V_\mu + A_\mu | B_i \rangle = C u_{B_f}(p') \Big[f_1(q^2)\gamma_\mu + i\frac{f_2(q^2)}{m_1 + m_2}\sigma_{\mu\nu}q^\nu + \frac{f_3(q^2)}{m_1 + m_2}q_\mu
$$
$$
+ g_1(q^2)\gamma_\mu\gamma_5 + i\frac{g_2(q^2)}{m_1 + m_2}\sigma_{\mu\nu}q^\nu\gamma_5 + \frac{g_3(q^2)}{m_1 + m_2}q_\mu\gamma_5 \Big] u_{B_i}(p).
$$
$$
(20)
$$

The factor C here is the Cabbibo factor. At low transferred momenta only two terms, f_1 (vector) and g_1 (axial vector), become important. It is customary to extract the experimental value $g_A/g_V = g_1(0)/f_1(0)$. The operators for the Fermi transitions $(d \rightarrow u)$ and Gamov–Teller transitions $(s \rightarrow u)$ can be expressed in terms of the SU(3) group generators

$$
A_\mu^{1+i2} = \gamma_\mu\gamma_5[T^1 + iT^2] \text{ and } A_\mu^{4+i5} = \gamma_\mu\gamma_5[T^4 + iT^5]. \quad (21)
$$

The semi-leptonic decays can be well described assuming the so-called SU(3) model. In this model the matrix elements of the vector current can be calculated without any free parameters. The matrix elements of the axial-vector currents can be expressed in terms of two parameters, denoted as F and D.

Mesonic corrections lead to the renormalization of the axial-vector coupling constants. The vector coupling constants are protected against renormalization by vector current conservation. Mesonic corrections to the axial-vector coupling constant can be taken into account by calculating the loop
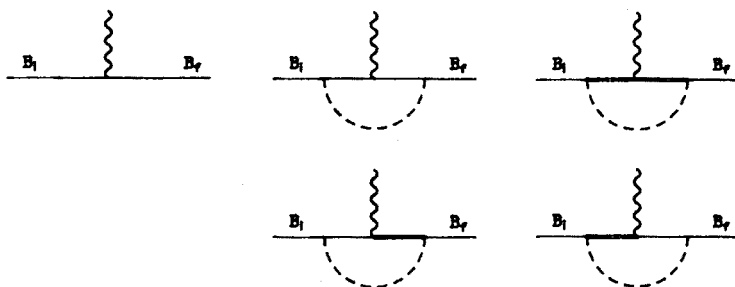
Fig. 5. Diagrams for the axial-vector current matrix elements. The single solid lines correspond to the octet baryons, the double solid lines to the decuplet baryons, and the dashed lines to the pseudoscalar mesons.

corrections to the tree level approximation (see Fig. 5). Here we report on the results with the inclusion of intermediate pseudoscalar mesons and associated octet and decuplet baryons only (the calculations with inclusion of vector mesons are in progress and will be presented elsewhere [17]).

In this section and in the next one we use a slightly different technique. Instead of the covariant method of Ref. [10] we use the light cone method proposed recently [16, 22]. The advantage of the method is that it guarantees local gauge invariance and energy-momentum sum rules automatically. The essence of the method is a use of form factors which fulfill certain symmetries. In terms of the invariant mass of the intermediate system MB they read as

$$G_{MB/N} = \exp \left[\frac{m_N^2 - m_{MB}^2}{2\Lambda^2} \right] . \tag{22}$$

The form factors commonly used in the traditional nuclear physics do not guarantee the required symmetries.

In contrast to the problems discussed in the previous sections, the axial-vector current matrix elements are very sensitive to the details of the model. This requires very careful analysis of the model parameters. Here the form factors of the vertices are especially important. The cut-off parameters of the form factors (22) have been fixed by fitting to the high energy data: $p(p,n)X$, $p(p,\Lambda)X$ and $p(p,\Delta^{++})X$ (details will be presented in Ref. [17]).

Including the diagrams shown in Fig. 5 and assuming the SU(3) symmetry for axial-vector currents, there exist 4 independent coupling constants: F and D for the transitions between the octet baryons, g_{10-10} for the transitions within the decuplet of baryons, and $g_I = g_{8-10} = g_{10-8}$ for the mixed transitions (interference diagrams). In order to reduce number of free parameters g_{10-10} and g_I have been fixed to their SU(6) values and, as in the case of the simple SU(3) fit, only F and D have been fitted to the experimental data on g_A/g_V. The obtained values of F and D are not

far from the SU(6) limit ($F = 0.47, D = 0.91$ compared with $F = 0.44$, $D = 0.82$ in the pure SU(3) fit). The resulting values of g_A/g_V are compared in Table II with the SU(6) tree results and that obtained in the SU(3) tree model with parameters fitted to the semileptonic decay data. The χ^2 values presented in Table II give an idea of the fit quality. The quality of the fit within our model is very similar to that obtained within the traditional SU(3) fit. It would even improve with allowance for the variation of g_{10-10} and g_I. A completely unrestricted fit could result, however, in unphysical values of parameters due to very limited number of experimental data.

TABLE II

The value of g_A/g_V in different models in comparison with the experimental data.

decay	SU(6)	SU(3)	our model	experiment
1. $n \rightarrow p$	1.67	1.26	1.25	1.2573 ± 0.0028
2. $\Sigma^- \rightarrow \Lambda$	0.82	0.67	0.72	0.6000 ± 0.0300
3. $\Lambda \rightarrow p$	-1.22	-0.87	-0.88	-0.8570 ± 0.0180
4. $\Xi^- \rightarrow \Lambda$	0.41	0.20	0.20	0.3100 ± 0.0600
5. $\Sigma^- \rightarrow n$	0.33	0.38	0.42	0.3400 ± 0.0500
χ^2/N	4369	2.00	4.90	

6. Spin structure of the nucleon

In recent years there has been much excitement about polarised deep-inelastic scattering [23, 24]. After a Regge extrapolation of the deep-inelastic structure function $g_1^p(x)$ to $x = 0$, EMC found

$$S_{EJ}^p = \int_0^1 g_1^p(x)dx = 0.126 \pm 0.010(\text{stat}) \pm 0.015(\text{syst})\,. \qquad (23)$$

In the parton model of Feynman g_1^p can be expressed as

$$g_1^p(x) = \tfrac{1}{2} \left[\tfrac{4}{9}\Delta u(x) + \tfrac{1}{9}\Delta d(x) + \tfrac{1}{9}\Delta s(x) \right]\,, \qquad (24)$$

where $\Delta q_f(x) = q_f^\uparrow(x) - q_f^\downarrow(x)$. The quantity

$$g_A^0 = \Delta u + \Delta d + \Delta s\,, \qquad (25)$$

determines the fraction of the proton spin which is carried by its quarks. The result (23) combined with semileptonic decay data yields a most surprising result

$$g_A^0 = 0.120 \pm 0.094(\text{stat}) \pm 0.138(\text{syst})\,, \qquad (26)$$

which is consistent with zero. This result is often called the proton spin crisis. The experimental result has inspired one of the most serious debates in the last decade about the theoretical interpretation of the spin and its connections to QCD. Here we concentrate only on the classical part of the problem in the framework of our meson cloud model of the nucleon.

The parameters fixed in the previous section can be used to estimate the effect of the meson cloud on the spin structure of the nucleon. The matrix elements of the flavor singlet axial-vector current can be calculated analogously to those for the semileptonic decays.

TABLE III

Quark polarizations, the Ellis–Jaffe sum rules for proton and neutron and the Bjorken sum rule in the SU(6) model and in our meson cloud model (MCM).

model	Δu	Δd	Δs	g_A^0	S_{EJ}^p	S_{EJ}^n	S_B
SU(6)	4/3	−1/3	0.000	1.000	5/18	0.000	5/18
MCM (SU(6))	1.128	-0.326	0.002	0.804	0.233	−0.009	0.242
MCM (SU(3))	0.858	-0.399	0.001	0.461	0.169	−0.041	0.210

In Table III we compare the results of our model with those in the classical SU(6) model, so successful in the description of the neutron-to-proton magnetic moment ratio. As seen from the table, the meson cloud model predicts a strong reduction of the spin carried by quarks in comparison to the naive SU(6) model. In addition to S_{EJ}^p we present the Ellis–Jaffe sum rule for the neutron S_{EJ}^n and the Bjorken sum rule S_B. Although we get a strong reduction from the $5/18$ of the SU(6) model for the S_{EJ}^p, the meson cloud model alone cannot account for the experimentally measured value. Obviously other effects, such as those discussed in Ref. [25], must play an important role. The effect of the meson cloud cannot, however, be neglected in the total balance of the proton spin. As far as S_{EJ}^n is considered, the experiments at CERN and at SLAC are under way. Recently some preliminary results have been announced [26]. The value of S_{EJ}^n and S_B obtained in our model are consistent with those obtained by SMC [26]:

$$S_{EJ}^n = -0.08 \pm 0.04(\text{stat}) \pm 0.04(\text{syst}), \tag{27}$$

$$S_B = 0.20 \pm 0.05(\text{stat}) \pm 0.04(\text{syst}). \tag{28}$$

7. Conclusions

In the light of recent experiments on the deep-inelastic muon scattering by nucleons, the understanding of the nucleon structure has become one of

the most intriguing problems of particle and nuclear physics. The recent observation of the Gottfried Sum Rule violation suggests a flavor asymmetry of the light sea quarks in the nucleon. Although the asymmetry does not contradict any fundamental principles, the flavor symmetry of the nucleon sea had become a part of the folklore in the particle physics community.

An asymmetry occurs in a natural way within certain non-perturbative models of the nucleon, built with valence quarks surrounded by a meson cloud. There exist two classes of models of this type. In the chiral quark model [8] the mesons are directly coupled to quarks. In the model discussed in the present paper, the nucleon is regarded as a quark core surrounded by the meson cloud. This picture of the nucleon provides a good description of nucleon electric polarizabilities [27]. It also has a close connection to models of low-energy hadron–hadron scattering [28, 29]. The value for the Gottfried Sum Rule is almost in agreement with that obtained by NMC.

In contrast to phenomenological parametrizations of the $\bar{d}$-$\bar{u}$ asymmetry, the meson cloud model discussed here predicts asymmetry concentrated at small x, quite similar to a recent fit [12] to the world data for DIS and Drell–Yan processes. As a consequence, the model predicts only 10%-20% deviations to be observed in a Fermilab experiment [30] measuring the relative dilepton yield in proton–proton and proton–deuteron Drell–Yan processes.

The mesonic corrections lead to the renormalization of the axial-vector current matrix elements, which seems to be unwanted in the light of the success of the simple Cabibbo theory. Large one-loop corrections to g_A, which explicitly violate SU(3) symmetry, can be compensated by a shift in the values of the symmetric (D) and antisymmetric (F) axial coupling constants. It appears accidental that values for D and F, consistent with experimental data, can be obtained in both the SU(3) fit and by the inclusion of the meson cloud.

We get a significant flow of the nucleon spin to the angular momentum of the mesonic cloud. Although the meson cloud model does not reproduce completely the EMC result for the Ellis–Jaffe sum rule, the contribution of the meson cloud cannot be neglected in the total balance of the proton spin.

REFERENCES

[1] K. Gottfried, *Phys. Rev. Lett.* **18**, 1174 (1967).
[2] P. Amaudruz *et al.*, *Phys. Rev. Lett.* **66**, 2712 (1991).
[3] D.A. Ross, C.T. Sachrajda, *Nucl. Phys.* **B149**, 497 (1979).

[4] E.M. Henley, G.A. Miller, *Phys. Lett.* **251B**, 453 (1990).
[5] A. Signal, A.W. Schreiber, A.W. Thomas, *Mod. Phys. Lett.* **A6**, 271 (1991).
[6] W. Melnitchouk, A.W. Thomas, A.I. Signal, *Z. Phys.* **A340**, 85 (1991).
[7] S. Kumano, J.T. Londergan, *Phys. Rev.* **D44**, 717 (1991).
[8] E. Eichten, I. Hinchliffe, C. Quigg, *Phys. Rev.* **D45**,2269 (1992).
[9] W-Y.P. Hwang, J. Speth, G.E. Brown, *Z. Phys.* **A339**, 383 (1991).
[10] A. Szczurek, J. Speth, *Nucl. Phys.* **A555**, 249 (1993).
[11] S.D. Ellis, W.J. Stirling, *Phys. Lett.* **256B**, 258 (1991).
[12] A.D. Martin, W.J. Stirling, R.G. Roberts, *Phys. Rev.* **D47**, 867 (1993).
[13] G.G. Arakelyan, A.A. Grigoryan, *Sov. J. Nucl. Phys.* **34**, 745 (1981).
[14] D. Brick *et al.*, *Phys. Rev.* **D21**, 632 (1980).
[15] E.G. Boos *et al.*, *Nucl. Phys.* **B151**, 193 (1979).
[16] V.R. Zoller, *Z. Phys.* **C53**, 443 (1992).
[17] H. Holtmann, A. Szczurek, J. Speth, paper in preparation.
[18] S.D. Drell, T.M. Yan, *Ann. Phys.* **66**, 578 (1971).
[19] J.F. Owens, *Phys. Lett.* **266B**, 126 (1991).
[20] D.M. Alde *et al.*, *Phys. Rev. Lett.* **64**, 2479 (1990).
[21] R.D. Field, R.P. Feynman, *Phys. Rev.* **D15**, 2590 (1977).
[22] V.R. Zoller, ITEP preprint, ITEP-80-92 (1992).
[23] J. Ashman *et al.*, *Phys. Lett.* **206B**, 364 (1988).
[24] J. Ashman *et al.*, *Nucl. Phys.* **B328**, 1 (1989).
[25] R.L. Jaffe, A. Manohar, *Nucl. Phys.* **B337**, 509 (1990).
[26] B. Adeva *et al.*, (SMC), *Phys. Lett.* **302B**, 533 (1993).
[27] V. Bernard, N. Kaiser, U.G. Meissner, *Nucl. Phys.* **B373**, 346 (1992).
[28] R. Machleidt, K. Holinde, Ch. Elster, *Phys. Rep.* **149**, 1 (1987).
[29] B. Holzenkamp, K. Holinde, J. Speth, *Nucl. Phys.* **A500**, 485 (1989).
[30] G.T. Garvey *et al.*, FNAL proposal, P866 (1992).
[31] P.L. McGaughey *et al.*, *Phys. Rev. Lett.* **69**, 1726 (1992).